Catalysis Today 143 (2009) 293–301

Contents lists available at ScienceDirect

Catalysis Today

journal homepage: www.elsevier.com/locate/cattod

# Characterization of zeolite basicity using probe molecules by means of infrared and solid state NMR spectroscopies

Manuel Sánchez-Sánchez [1], Teresa Blasco *

*Instituto de Tecnología Química (UPV-CSIC), Avda. de los Naranjos s/n, 46022-Valencia, Spain*

ARTICLE INFO

*Article history:*
Available online 22 January 2009

*Keywords:*
Zeolite basicity
Probe molecules
NMR
Infrared
Pyrrole
Chloroform
Methanol
Methoxy
Nitrosonium
Chlorodifluoromethane

ABSTRACT

This work reviews the use of pyrrole, chloroform, methanol, as well as methoxy and nitrosonium groups generated 'in situ', as infrared and NMR probe molecules to characterize zeolites basicity. The main results reported in the bibliography about the correlation of the spectroscopic properties of the adsorbed molecule with the framework basicity, the host–guest interactions, and the limitations in the use of these molecules as probes for zeolite basicity are discussed. Special attention is paid to the results reported for the adsorption of pyrrole and halocarbons, most specially $CHCl_3$ and $CHClF_2$ over alkali-exchanged FAU-type zeolites using IR and NMR spectroscopies.

## 1. Introduction

Aluminosilicate zeolites possess negatively charged framework which can be compensated by protons, forming bridging hydroxyl groups with Brønsted acidity; or by alkaline cations, conferring the zeolites basic properties. The high economical impact of petrochemical processes catalysed by acids has prompted a large activity research on the characterization and applications of acidic zeolites, and the development of novel structures with new pore dimensions, topologies and composition [1,2]. Meanwhile, the investigation of the properties and catalytic applications of basic zeolites has been limited so far, despite the numerous base catalysed reactions of commercial interest which could be potentially processed [2–6]. Although an increased attention has been paid since the mid eighties, there are still place to better exploit the application of basic zeolites as catalysts [2–6], adsorbents and in gas separation processes [7–10]. Their properties will be determined by the strength, population and distribution of the basic sites, and their accessibility to reactant and adsorbate molecules. Therefore, a full characterization of basic zeolites is desirable in order to understand their performance as sorbents and catalysts and to design materials optimized for a given application.

Intrinsic zeolites basicity is of Lewis type and resides on the framework oxygen atoms bearing the negative charge, increasing as the framework Al content increases (the Si/Al molar ratio decreases) [3,4,11]. For a given Si/Al ratio, the negative charge on the oxygen atoms is enhanced as the electropositive character of the nonframework compensating cations increases; considering the series of alkaline cations, the zeolite basicity increases in the order: $Li^+ < Na^+ < K^+ < Rb^+ < Cs^+$ [3,4,11]. The average negative charge on the oxygen atoms can be estimated by the application of the Sanderson electronegativity equalization method from the zeolite chemical composition [11]. The basicity of zeolites was initially interpreted as a property of the whole solid [12] but later, experimental and theoretical results suggested that it also depends on the structure and on the local environment of the basic site [11,13–15].

The most common approach to characterize zeolite basicity involves the use of probe molecules whose physico-chemical properties are modified by the interaction with the basic sites and measured by the appropriate techniques [3–5]. Common molecules used as probes for basic sites in zeolites usually posses an acidic proton which is able to form hydrogen bonds with the basic framework oxygen atoms [3–5,11,12,14–16]. This produces the polarization of the molecule bond in an amount which depends on the basic strength of the site, and can be measured by a spectroscopic technique, more usually, by infrared spectroscopy [3–5,11,12,14,16]. Among the adsorbate used as probes, special

---

* Corresponding author. Tel.: +34 963877812; fax: +34 963877809.
*E-mail address:* tblasco@itq.upv.es (T. Blasco).

[1] Present address: Instituto de Catálisis y Petroleoquímica, CSIC, C/ Marie Curie 2, 28049 Madrid, Spain.

0920-5861/$ – see front matter © 2008 Elsevier B.V. All rights reserved.
doi:10.1016/j.cattod.2008.12.012

attention has been paid to pyrrole [11,12,14–22], chloroform [16,23–30] and methanol [31–36]. Meanwhile, alternative methods use in situ generated species, such as $CH_3^+$ [37–41] or $NO^+$ (nitrosonium) [42–47] which links to the basic oxygen atoms of the zeolite framework. Besides infrared, other spectroscopic techniques such as XPS [15,24] and NMR [21,22,25–27,35,37–40,48–50] have been used to monitor the modifications of the molecule properties induced by interaction with basic zeolites.

An ideal acidic probe molecule should interact exclusively with the zeolite basic lattice oxygens. However, these are close to compensating alkaline cations whose acid strength follows the opposite trend than the oxygen basicity, i.e., decreases as the Al content in the network increases, and for the alkali series, in the order: $Li^+ > Na^+ > K^+ > Rb^+ > Cs^+$ [11]. Therefore, different individual atoms or groups of atoms of a probe molecule can simultaneously interact with the network oxygen and with its conjugated acid cation site [19–22,25–26,28–30]. The difficulty to elucidate the effect of both interactions on the property measured may question the validity of some molecules to be used as probes for zeolite basicity, being required a deep understanding of the interaction between the adsorbate and the zeolite lattice.

In this paper, we summarize the results reported on the host–guests interactions of the most studied probe molecules, i.e., pyrrole, chloroform and halocarbons, and methanol, as well as methoxy and nitrosonium groups, with the basic zeolite lattice. Special attention is paid to the results obtained by our group upon adsorption of pyrrole [21,22,48] and halocarbons [26,49,50] on alkali-exchanged FAU-type zeolites, combining infrared and NMR spectroscopies.

## 2. ‘In situ’ generated probe molecules for zeolites basicity

Methoxy and nitrosonium groups generated ‘in situ’ become directly attached to lattice zeolite oxygen acting as probes of zeolite basicity. According to scheme (1), methoxy groups are formed by the bonding to the framework oxygen of the methyl group released upon the chemisorption of methyl halides, usually $CH_3I$ [37–40], on zeolites:

$$CH_3I + M^+ \, {}^-O\langle Z \rightarrow CH_3O - Z + M^+ I^- \qquad (1)$$

where ${}^-O\langle Z$ represents a zeolite framework oxygen.

Various methyl halides have been used to generate methoxy groups, in a concentration which depends on the halogen and follows the trend: $CH_3I > CH_3Br > CH_3Cl$ [51]. The removal of the halide is assisted by the metal, being favoured on hard, more acidic cations associated to less basic framework oxygen, which are more difficult to be methylated [41]. The halogen–cation and the methyl–oxygen interactions compete in the activation energy of the process, prevailing the latter for methyl iodide [41]. The $^{13}C$ NMR chemical shift of the methoxy groups depends on the strength of the interaction with the lattice oxygen, which increases with the zeolite basicity [37–40]. Bosáček et al. [37,38] found a linear correlation between the $\delta^{13}C$ of surface bonded methoxy $^{13}CH_3O\langle Z$ and the mean Sanderson electronegativity of the zeolite framework oxygens. $\delta^{13}C$ of methoxy shifts to high field, i.e., the carbon becomes more shielded, as the oxygen basicity increases, varying between 58.7 ppm for NaZSM-5 (Si/Al = 22.4) and 54 ppm for the basic CsX zeolite [37,38]. The methoxy groups generated in the zeolite by this method react above 440 K to give hydrocarbons, but they are perfectly stable under the conditions they are used as probes for zeolite basicity [51].

More recently, another molecule generated in situ, the ion nitrosonium has been suggested to be a good infrared probe molecule for zeolite basicity. Thibautl-Starzyk et al. [42,43] have shown that the vibration frequency of surface adsorbed $NO^+$, $\nu(NO^+)$, is sensitive to the negative charge of the lattice oxygens of zeolites.

Nitrosonium cations ($NO^+$) are formed in alkali-exchanged zeolites by disproportionation of the $N_2O_4$ dimer, as shown in scheme (2):

$$N_2O_4 + M^+ \, {}^-O\langle Z \rightarrow NO^+ \, {}^-O{-}Z + M^+ NO_3^- \qquad (2)$$

The reaction generates nitrosonium and nitrate ions that remain closely; the nitrate reacts with the alkaline cations and the $NO^+$ interacts directly with the negatively charged lattice oxygen atoms [42,43,52]. Theoretical results indicate that there is a cooperative influence of the extraframework cations and the confinement effects of the zeolite matrix in the disproportionation of $N_2O_4$ over alkali-exchanged faujasites [46]. This reaction requires a cation at a site SIII [47], and then, the mobility of the extraframework cations induced by adsorption is essential for $N_2O_4$ disproportionation [46,47].

The oxygen transfers electron density to the $\pi^*$ antibonding orbital of the adsorbed nitrosonium, modifying the infrared stretching vibration frequency $\nu(NO^+)$, which is sensitive to the negative charge on the zeolitic oxygen atom. In this way, infrared spectroscopy of adsorbed $NO^+$ allows to differentiate oxygen atoms located in the main channels or in the side pockets of mordenite [52]. In basic faujasites, the spectra show overlapping $\nu(NO^+)$ bands corresponding to the several possible locations and/or to adsorption sites with different number of nearby aluminum tetrahedra or sodium atoms [42–44]. The stretching frequency of the band ascribed to $NO^+$ adsorbed on supercage positions increases with the chemical hardness (acidity) of the cation giving a good linear correlation, especially for zeolites X [42–45].

The stretching frequency of adsorbed $NO^+$ has been claimed to correlate well with the zeolite basicity, decreasing as the negative charge on the oxygen increases [42–44]. The $\nu(NO^+)$ is red-shifted in $180\ cm^{-1}$ when the zeolite basicity increases from partially exchanged LiX to RbX zeolites, appearing as a sensitive probe for zeolite basicity [42–44]. Computed frequencies follow the expected trends: irrespective of the alkali, all zeolites X are more basic than zeolites Y; and for both, the basicity increases from $Na^+$ to $K^+$ and to $Rb^+$ [47]. However, these results disagree with the experimental ones since, according to the $\nu(NO^+)$ frequency, the oxygen basicity decreases in the order: RbX > KX > RbY > KY > NaX > NaY > LiX > LiY [42,43]. This trend is unexpected since zeolites X are more basic than zeolites Y and indeed, calculated frequencies for zeolites X are sensibly higher than the experimental ones [47]. As a result, the correlation between the $\nu(NO^+)$ and the negative charges on the lattice oxygen calculated by the Sanderson electronegative equalization method, shown in Fig. 1, is very poor.

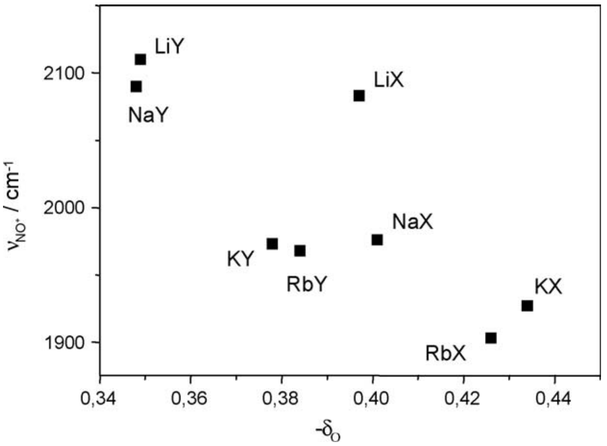

**Fig. 1.** Correlation of the stretching frequency of $NO^+$, $\nu_{NO}$, adsorbed on different alkali-exchanged FAU-type zeolites versus the mean negative charge on the lattice oxygen atoms calculated by the electronegativity equalization method, after Refs. [42,43].

The results summarized above indicate that $\nu(NO^+)$ correlates very poorly with the zeolite basicity, and well with the cation chemical hardness despite this is not directly involved on the $NO^+$ adsorption but occupying nearby positions [42,43]. Indeed, the discrepancies found between experimental and computed frequencies led to the conclusion that a systematic study of the number and distribution of aluminum tetrahedra is necessary to see what the effect is on the NO frequencies and on the basicity [47].

No further reaction or decomposition of $NO^+$ on basic zeolites has been reported, and far from that, this ion has been described as the most stable $NO_x$ species in these materials [53]. However, $NO^+$ reacts with $N_2O_4$ in presence of water to give nitric acid [53,42].

## 3. Probe molecules forming hydrogen bonds with framework oxygen atoms of zeolites

Besides the requirements mentioned in the introduction, a probe molecule for zeolite basicity must keep its integrity under the experimental conditions used. As mentioned above, this is true for nitrosonium and methoxy ions, as well as for the molecules discussed in this paragraph, i.e., pyrrole, halocarbons, and methanol, though some of them can give reactions under certain conditions. More specifically, pyrrole can polymerize on zeolite acid sites [14,15(b),54,55] or dissociate on metallic oxides [56–58], but no reaction has been reported on basic zeolites even after desorption at 523 K [48(b)]. Chloroform may decompose on some basic solids [59,60], and reacts with basic zeolites at moderate temperatures [61], but the reaction is negligible at room temperature for several days [26]. Chlorodifluoromethane reacts with the aluminium from the zeolite framework above 470 K [62], but no extra compound has been detected by NMR after adsorption at room temperature on basic faujasites [50]. Finally, methanol has been reported to form dimethyl ether on basic zeolites at temperatures above 400 K, but no reactivity has been observed at room temperature [63,64].

### 3.1. *Pyrrole*

#### 3.1.1. *The hydrogen bonding of pyrrole with framework oxygen atoms*

Pyrrole was used to characterize zeolite basicity for the first time by Scokart and Rouxhet [12] in the beginning of the eighties, and is the most studied amongst the proposed acidic probe molecules. The –NH group of pyrrole interacts with the framework oxygen atoms forming bridges and polarizing the –NH bond. As a consequence, the infrared NH stretching frequency ($\nu_{NH}$) shifts to lower wavenumbers as the basicity of the site increases [11,12]. In the former publication [12], zeolite basicity was considered to be a collective property of the solid. Later on, the coexistence of two –NH vibration bands [14] and two $N_{1s}$ XPS peaks [15] led to conclude that the basicity of the sites was mainly determined by the local environment rather than by the bulk composition.

Barthomeuf [11] studied the basicity of various zeolites possessing different structures and chemical compositions, assuming that pyrrole must be adsorbed over basic oxygen of the zeolitic rings in the large cages where cations are placed. The $\nu_{NH}$ of pyrrole was shown to correlate with the mean negative charge on the framework oxygen atoms calculated by the Sanderson equalization method [11]. One of the main conclusions reached was that this correlation is highly structure dependent, and only zeolites of the same topology can be compared, which was explained by differences in the cation arrangement in the oxygen rings [11]. This and the dual acid–base character in the cationic zeolites have to be taken into account when considering the interaction with the adsorbate [11]. Most recently, Barthomeuf [13] has described the basicity of cation exchanged zeolites using topological clusters, showing the importance of the framework Al location and topology.

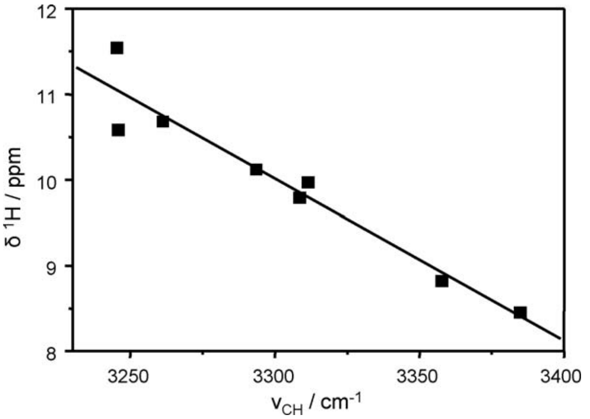

**Fig. 2.** Correlation of the average stretching frequency, $\nu_{NH}$, versus $\delta^1H$ of the NH group of pyrrole adsorbed at room temperature and subsequently desorbed at 338 K on different alkali-exchanged FAU-type zeolites.

The coexistence of two bands in the IR and XPS spectra of pyrrole over alkali-exchanged zeolites was attributed to molecules adsorbed on lattice oxygen atoms adjacent to different type of cations [14,15]. The presence of several –NH components evidenced by computer deconvolution of the broad infrared NH stretching bands supported the basic site heterogeneity on partially alkali-exchanged EMT zeolites [17]. It was assumed that chemisorbed pyrrole forms a collinear bonded complex with basic framework oxygen atoms ($C_4H_4NH\cdots O_{zeol}$), and that the cation influences only the adjacent framework oxygen atoms [14,15(a),17]. The average $\nu_{NH}$ value obtained from the simulated spectra showed a better correlation with the negative charge on the framework oxygen atoms than the band maxima [17]. Meanwhile, differences between bulk and local chemical composition where taken into account calculating the local negative charge of the oxygen atoms by the Sanderson method [14,15].

Pyrrole has been used as an NMR probe molecule to measure zeolite basicity; the $^1H$ chemical shift of the –NH group shifts up to 3 ppm to low field as the zeolite basicity increases from LiY to CsX [21]. None site heterogeneity is evident by $^1H$ NMR since the spectra show a unique –NH peak because of the longer time scale as compared with infrared spectroscopy [21]. Fig. 2 shows that $^1H$ NMR chemical shifts correlate well with the average $\nu_{NH}$ frequencies calculated from the decomposition of the infrared –NH stretching band. Therefore, the $^1H$ NMR chemical shift of pyrrole adsorbed over FAU-type zeolites is a good measurement of the average zeolite basicity [21].

#### 3.1.2. *The interaction of pyrrole with exchanged alkaline cations*

Theoretical calculations on the adsorption of pyrrole on FAU-type zeolite at low loading led to the model depicted in Fig. 3, in which the pyrrole ring interacts only with cations at SII sites and the NH group points into the direction of framework oxygen O4 [19] or O1 [20]. Pyrrole was concluded to be a good probe for basic sites since the NH bond polarization increases according to the known trends of intrinsic zeolite basicity [19,20]. The adsorption model of Fig. 3, with a stoichiometry of one sorbate molecule per SII $Na^+$ cation, was found experimentally for zeolite NaY by XRD techniques [20]. Meanwhile, a more complex coordination is obtained for zeolite NaX, as two instead of one pyrrole molecule interact with a single sodium cation [20]. Indeed, theoretical calculation shows that the cation–ring interaction is the driving force for pyrrole adsorption on alkaline cations at SIII occupied in zeolites X [20,65].

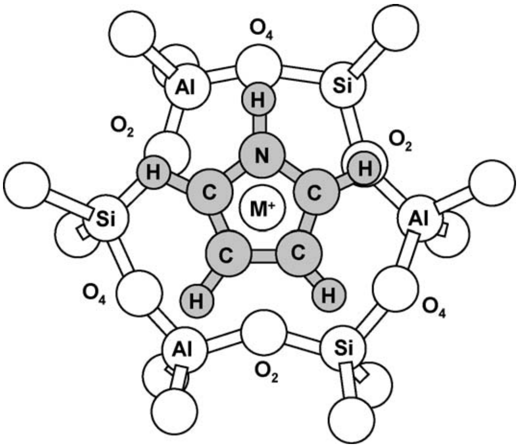

**Fig. 3.** Geometry of pyrrole adsorbed onto a cation $M^+$ at the SII position in a 3-Al hexagonal window (6-MR) of FAU-type zeolite, after Ref. [19].

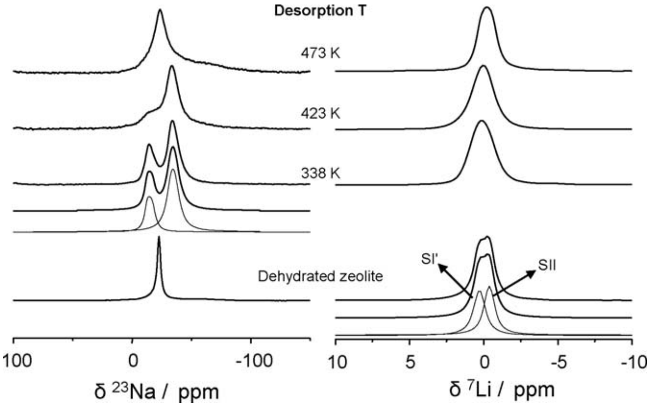

**Fig. 5.** $^{23}$Na (left) and $^7$Li (right) MAS NMR spectra of partially exchanged zeolite LiX bare (bottom) and after the pyrrole adsorption and subsequent evacuation at the indicated temperatures, after Ref. [48(b)]. The components and the simulations of the $^7$Li and $^{23}$Na spectra recorded for the LiX zeolite bare and after pyrrole desorption at 338 K, respectively, are displayed.

The investigation on the host–guest interactions by multinuclear solid state NMR [20,21,48] gives further experimental evidence of the models previously proposed by theoretical methods and XRD analyses for pyrrole adsorption on FAU zeolites [19,20]. The methodology used for commercial and partially exchanged Li-, K- and Cs-zeolites NaY and NaX and the main conclusions are illustrated here for partially exchanged Li faujasites [21,22,48(a)].

Fig. 4 shows the $^7$Li (right) and $^{23}$Na (left) MAS NMR spectra of partially exchanged zeolite LiY (chemical composition: $Li_{34}Na_{21}Si_{137}Al_{55}O_{384}$) degassed at 673 K and with different pyrrole contents [22]. The simulation of the $^7$Li and $^{23}$Na spectra of the dehydrated zeolite (not shown) leads to the following site population for $Li^+$: 24 SI′ and 10 SII; and for $Na^+$: 0.5 SI, 7.5 SI′ and 13 SII [22]. The spectra of the bare zeolite are sharply modified by the chemisorption of pyrrole at 338 K (see Fig. 4). The main $^7$Li NMR signal becomes symmetric and a new one appears at high field, which is attributed to $Li^+$ cations originally at sites SII interacting with the π electrons of the pyrrole ring. Therefore, SII $Li^+$ cations, non-accessible to gas molecules, may move out of the plane of oxygens to bind the pyrrole molecules. Also the $^{23}$Na NMR spectrum changes upon pyrrole adsorption at 338 K (see Fig. 4): the two large quadrupolar signals of sites SI′ and SII disappear, while a much narrower one attributed to supercage $Na^+$ interacting with the ring of pyrrole emerges. This result indicates that pyrrole adsorption provokes the migration of $Na^+$ from the sodalite units (SI′ sites) to the supercage. After degassing at 423 K, the original $^7$Li spectrum is practically recovered though some pyrrole remains in the zeolite, which must be selectively adsorbed over more electropositive $Na^+$ cations, since its spectrum is hardly modified (see Fig. 4) [22]. Meanwhile degassing at 473 K is required to completely desorb pyrrole and to recover the original $^{23}$Na spectrum. Quantification of chemisorbed molecules by integration of the $^1$H NMR spectra, and of interacting cations from $^7$Li and $^{23}$Na NMR spectra indicates that one pyrrole is interacting with one supercage cation, supporting the theoretical adsorption model in which one pyrrole molecule is adsorbed onto a SII cation [19,20].

Fig. 5 shows the $^7$Li and $^{23}$Na MAS NMR spectra recorded for the adsorption experiments of pyrrole on partially exchanged zeolite LiX (chemical composition: $Li_{57}Na_{29}Si_{106}Al_{86}O_{384}$). The simulation of the $^7$Li spectrum of the dehydrated zeolite indicates that of the 32 SI′ and 32 SII sites per unit cell, 28 and 29, respectively, are occupied by $Li^+$; meanwhile the spectrum of $^{23}$Na consists of a relatively sharp signal attributed to mobile $Na^+$ at SIII′ supercage positions. Fig. 5 shows that, unlike for LiY, $Li^+$ at SII sites in zeolite LiX do not move to interact with pyrrole, which could be tentatively explained by the weaker acidity of lithium in the more basic zeolite LiX [11]. The changes observed in the $^{23}$Na NMR spectra indicate that pyrrole is adsorbed only over more basic sites involving more electropositive $Na^+$ cations. Therefore, and in agreement with previous results obtained by XRD analysis, slightly different results are obtained for the adsorption of pyrrole over

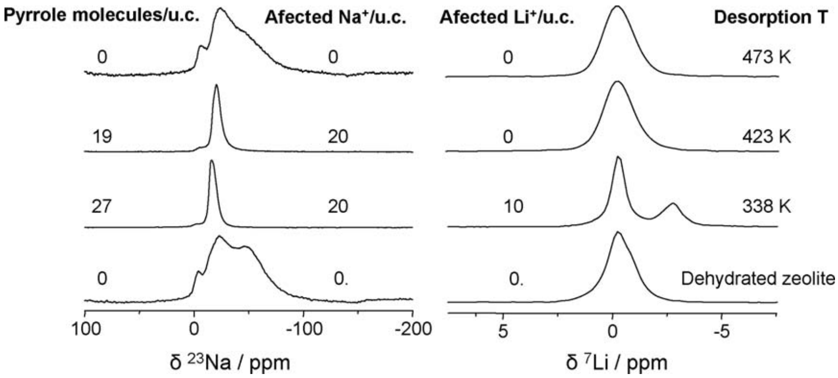

**Fig. 4.** $^{23}$Na (left) and $^7$Li (right) MAS NMR spectra of partially exchanged zeolite LiY bare (bottom) and after pyrrole adsorption at room temperature and subsequent evacuation at the indicated temperatures, after Refs. [21,22]. The number of pyrrole molecules/unit cell remaining in the zeolite after desorption at increasing temperature, indicated in the spectra, was measured by quantification of the $^1$H NMR spectra [22]. The number of $Li^+$ and $Na^+$ cations interacting with pyrrole, also indicated in the spectra, was determined from the NMR spectra [21].

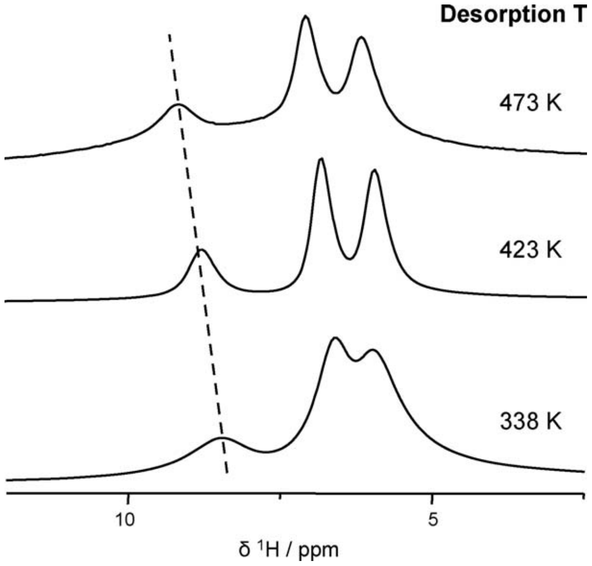

**Fig. 6.** $^{1}H$ MAS NMR of pyrrole adsorbed at room temperature and subsequently desorbed at the indicated temperatures on partially exchanged zeolite LiY, after Ref. [48(a)].

zeolites Y and X, probably because of the different population of alkaline cations in the supercage. Degassing at 473 K leads to the desorption of pyrrole and the practical recovering of the $^{23}Na$ NMR spectrum of the bare zeolite (see Fig. 5).

These results and those obtained for a series of partially exchanged alkali zeolite Y by multinuclear NMR spectroscopy, led to the following general conclusions [21,22,48]: (i) cations migrate from their original sites to accessible positions into the supercage to interact with the ring of pyrrole, in an extent which depends on the pyrrole loading; (ii) at lower loading, pyrrole is selectively adsorbed over sites associated with more electropositive cations.

### 3.1.3. *The origin of the basic site heterogeneity*

The site heterogeneity derived from the decomposition of the broad infrared NH stretching band of pyrrole chemisorbed on partially alkali-exchanged EMT zeolites was interpreted on the basis of the site cation population and the peaks intensity, assuming a collinear bonded complex ($C_4H_4NH\cdots O_{zeol}$) [17]. The origin of several components was attributed to molecules interacting with oxygen atoms adjacent to different type of alkaline cations at specific sites $I_a$, $I'_a$, $I'_b$ and II [17]. The interpretation of the spectra was made assuming [17]: (i) that all framework oxygen atoms in the supercage are accessible; (ii) no cation mobility in the presence of the adsorbed molecules at the very low coverage used; and (iii) that pyrrole adsorption preferentially occurs over more basic sites. A similar analysis was extended to partially exchanged alkali zeolites X and Y [18], and the components of the $\nu_{NH}$ infrared band were explained by the interaction of pyrrole with oxygen atoms adjacent to alkali cations at sites I′, I and II. For oxygen associated with $Na^+$ cations, the basic strength was reported to increase from sites I′ to I to II [18].

Theoretical calculations on the adsorption of pyrrole on faujasites [19,20] questioned the interpretation of the basic site heterogeneity given from infrared spectroscopy [17,18]. According to the calculated model, depicted in Fig. 3, only SII cations have a remarkable influence on the pyrrole molecule, and then, the contribution of several components to the NH infrared band was suggested to come from the heterogeneous Al distribution in the six-membered rings [19].

Fig. 6 shows the $^{1}H$ NMR spectra recorded after the adsorption of pyrrole at room temperature on partially exchanged zeolite LiY and subsequent desorption at increasing temperatures. The peak of the NH group progressively shifts to low field as the number of adsorbed molecules decreases, indicating that pyrrole is preferentially adsorbed over more basic sites. After degassing at 423 K, pyrrole is desorbed from the $Li^+$ sites, and the remaining molecules are adsorbed onto $Na^+$ (see Fig. 4), evidencing that more basic sites are associated with more electropositive cations. Similar NMR results were reported for zeolites LiX [48(a)] and NaX [48(b)], indicating the presence of basic oxygens of different strength in agreement with infrared results [17,18,22]. The existence of site heterogeneity in NaY and NaX indicates the influence of other factors besides the nature of the cation (vide infra). As previously suggested, a possible origin of the basic sites heterogeneity is the varying $AlO_4$ tetrahedra content in the six-membered rings where the cations are located, increasing the basicity with the aluminium content [19].

The NH infrared band of pyrrole adsorbed and subsequently desorbed at increasing temperatures on a series of partially exchanged zeolites Y was decomposed into different components [22]. The assignment of the individual bands was made taking into account the information obtained by NMR spectroscopy; this is illustrated in Fig. 7 for partially exchanged zeolite LiY (right) and for zeolite NaY (left). The IR NH band of all spectra are simulated with three components at constant frequencies corresponding to pyrrole adsorbed over six-membered rings containing 1, 2 or 3 Al atoms compensated by a $Na^+$ cation in position SII (see Fig. 7). An additional band of pyrrole adsorbed on the site involving $Li^+$ at site

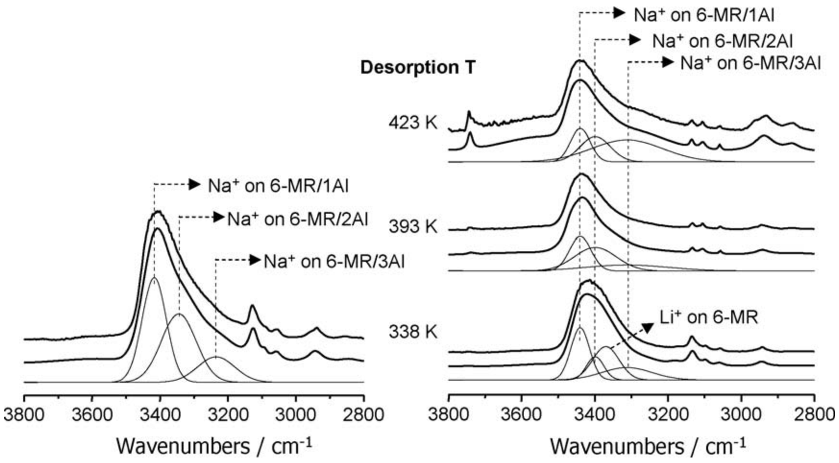

**Fig. 7.** NH stretching region of the FT-IR spectra after pyrrole adsorption at room temperature on NaY and subsequent desorption at 338 K (left), and on partially exchanged zeolite LiY after desorption at the indicated temperatures (right), after Ref. [22]. The band components and the simulated spectra are also shown.

SII is required to simulate the spectrum recorded for partially exchanged zeolite LiY after desorption at 338 K, in agreement with $^7$Li NMR studies [22]. Then, the pyrrole adsorption gives indirect information on the distribution of the $AlO_4$ tetrahedra in the framework of FAU zeolites [22]. The major effect of the distribution of $AlO_4$ tetrahedra in the zeolite basicity has been shown later by using basicity clusters [13].

## 3.2. Halocarbons

### 3.2.1. Chloroform

Since 1979 [66], chloroform has been used as a probe molecule in the characterization of solid basicity [60,66–69], though its use has been questioned because of its scarce sensitivity to the basic strength [69] and its decomposition over some particular basic centres [60]. Nevertheless, despite its reactivity within the zeolite at moderate temperatures has been made clear [26], there is a general agreement on its use as a probe for zeolite basicity [23–27].

The infrared stretching vibration frequency of the CH bond of adsorbed chloroform (or the CD bond for deuterated molecules) is red-shifted respect the neat compound in an extent which depends on the basicity of the host zeolite [23,25,26,70]. XPS studies concluded that chloroform is adsorbed on different zeolites by the acid–base interaction of the proton with the lattice oxygens [24], supporting its use as a probe to estimate the zeolite basicity. However, theoretical calculation [28–30,71], infrared spectroscopy [25] and calorimetric studies [29] suggested the simultaneous interactions of chlorine atoms with zeolite cations (electrostatic) [28–30,71] and with the lattice oxygen atoms (van der Waals) [28–30].

At the end of nineties, three different publications investigated the chloroform/FAU zeolite system by using NMR spectroscopy. One of them did not use the MAS technique, and consequently, the $^1$H spectra showed broad and overlapping signals, assigned to chloroform adsorbed on acid or on basic centres [27]. Bosch et al. [25] and our group [26] concluded that $\nu_{CH}$ as well as $\delta^1$H spectroscopic parameters can be adequately used as a measure of zeolites basicity. Meanwhile, $^{23}$Na NMR spectroscopy gave direct experimental evidence of the suggested simultaneous interaction between the chlorine atoms of chloroform and the alkaline cations [25,26].

The chloroform–cation interaction is illustrated in Fig. 8 for zeolite NaY, which displays the $^{23}$Na NMR spectra of the zeolite bare and containing 25 molecules of $CHCl_3$ per zeolite unit cell. The adsorption of chloroform provokes a decrease of the quadrupolar coupling constant (QCC) of accessible $Na^+$ cations, i.e., those located in the supercage (site SII), or near the supercage (position SI′) so that they can easily migrate to it [26,71]. The decrease of $^{23}$Na QCC is taken as an evidence of the halogen–cation interaction. This diminution is higher for pyrrole, which could suggest a weaker interaction of the alkaline cations with the halogen atoms of chloroform. However, the interaction of the cations with the $\pi$ electronic cloud of pyrrole is more delocalized and may increase the symmetry of the $Na^+$ environment, decreasing the quadrupolar character of the NMR signal, not necessarily involving stronger interaction than between Cl atoms and $Na^+$ cations.

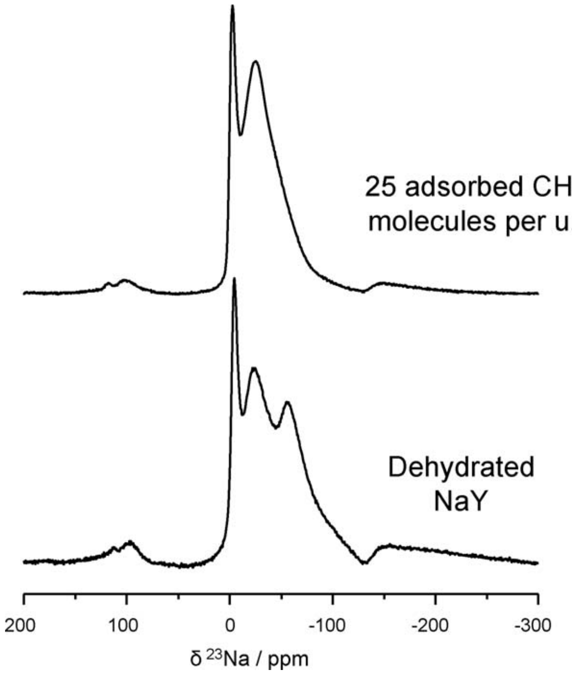

**Fig. 8.** $^{23}$Na MAS NMR spectra of zeolite NaY degassed at 673 K (bottom) and after adsorption of 25 molecules of chloroform per unit cell (top), after Ref. [26].

### 3.2.2. $CHF_3$ and $CHClF_2$

The reactivity of chloroform in zeolites at moderated temperatures prevents its use to determine the presence of basic sites of different strength by desorption at increasing temperatures [26]. A potentially suitable approach to characterize the number and strength of basic sites in zeolites is the combined use of probe molecules of varying acidity. In this sense, halocarbons of general formula $CHCl_{3-x}F_x$ ($0 \leq x \leq 3$) are particularly attractive because the proton acidity will decrease as the number of fluorine atoms in the molecule increases, while being similar from the structural point of view.

The acid character of $CHF_3$ has been proved to be too weak to form strong hydrogen bonds with the lattice oxygen atoms of alkali zeolites, and its adsorption is dominated by cation–fluorine interactions [25]. Therefore, though $^1$H NMR of this molecule behaves as that of chloroform, $CHF_3$ is less suitable as a probe for basic properties [25]. Some studies on the $CHClF_2$ adsorption over NaY [72] and alkali-exchanged ZSM-5 zeolites [62] suggested the involvement of cations and a systematic variation of $\delta^1$H with the $CHClF_2$ loading.

More recently, we have used $CHClF_2$ as an IR and NMR probe molecule to characterize the basicity of partially exchanged FAU-type zeolites [50]. As expected, the $\nu_{CH}$ stretching frequency of $CHClF_2$ shifts to lower frequencies as the basicity of the zeolites increases. However, the correlation with the negative charge on the framework oxygen atoms calculated by the Sanderson method is quite poor, probably because of the contribution of the halogen–cation interaction (vide infra) [50]. However, a better correlation, comparable to that reported for $CHCl_3$, is found when the $^1$H NMR chemical shift instead of $\nu_{CH}$ of adsorbed $CHClF_2$ is plotted, as shown in Fig. 9. $\delta^1$H of $CHClF_2$ and $CHCl_3$ change in about 1 ppm from the less basic LiY to the more basic KX zeolites, while for pyrrole, $\delta^1$H varies as much as 3 ppm [21] for the same zeolites, presumably due to its stronger acid character.

The linear correlation of $\delta^1$H and $\nu_{CH}$ of $CHClF_2$, $CHF_3$, and $CHCl_3$ with the negative density charge on the zeolite oxygen atoms suggests that these molecules are valid infrared and NMR probes for zeolite basicity [25,50]. Without any space constrains, less chlorodifluoromethane than chloroform should be adsorbed on the same zeolite because the lower acidity of the former. However, quantification of the proton NMR spectra shows that this is not the case, giving an indirect evidence of the contribution of the cation–halogen interactions [50,73].

### 3.2.3. The cation–halogen interaction: adsorption of $CHClF_2$

The occurrence of the cation–halogen interaction has been proved for $CHClF_2$ by solid state NMR, taking advantage of the

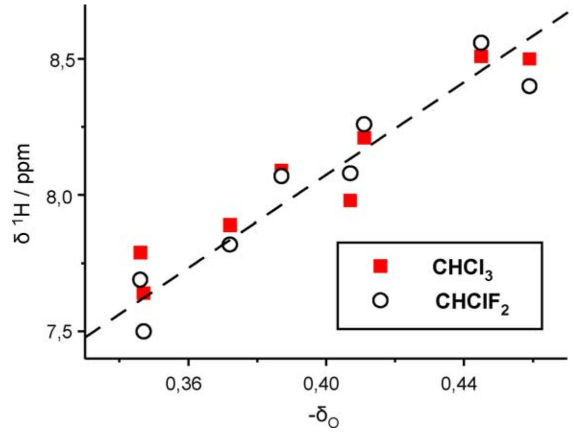

**Fig. 9.** Correlation of $\delta^1$H of CHClF$_2$ and CHCl$_3$ adsorbed on ion-exchanged FAU-type zeolites versus the mean negative charge over the framework oxygen $-\delta_O$ as determined by Sanderson's method, after Ref. [50].

nuclear magnetic properties of the $^{19}$F isotope (100% abundant, high NMR sensitivity and long-range of chemical shifts).

Fig. 10 shows the $^{19}$F MAS NMR spectra of CHClF$_2$ adsorbed over the commercial and partially alkali-exchanged zeolites NaX and NaY. All spectra consist of a doublet of the spin–spin coupling of $^{19}$F with the $^1$H through two chemical bonds $^2$J(F, H) [50]. Inspection of Fig. 10 indicates that $^{19}$F chemical shift is not determined by the zeolite basicity and that it is influenced by the nature of the cation [50]. $\delta^{19}$F of CHClF$_2$ adsorbed on partially exchanged Cs and K-zeolites Y and X are low-field shifted respect to free CHClF$_2$, in agreement with the expected higher electron withdraw of more electropositive cations [50]. Moreover, $^{19}$F chemical shift is similar for zeolites KY and KX, and for zeolites CsY and CsX, irrespective of the Si/Al ratio [50].

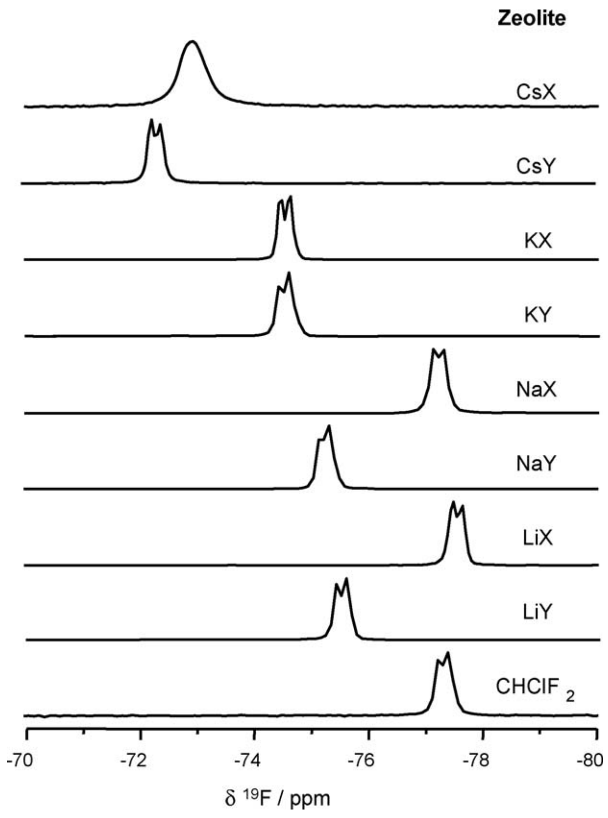

**Fig. 10.** $^{19}$F MAS NMR spectra of alkali-exchanged FAU-type zeolite after adsorption of 30 molecules CHClF$_2$ per unit cell, after Ref [50].

A different situation is observed for zeolites containing Li$^+$ and Na$^+$ as compensating cations, since $\delta^{19}$F CHClF$_2$ is dictated by the Si/Al ratio; therefore, this is similar for zeolites Y and for zeolites X, suggesting significantly weaker cation–fluorine interactions [50]. Though partially exchanged zeolites LiY and NaY do not chemisorb CHClF$_2$ at room temperature, the low field shift of $\delta^{19}$F respect to the free molecule points out that fluorine–cation interaction must occur to some extent; in LiY, the halogen must probably interact selectively with more basic sites involving Na$^+$ [50]. $\delta^{19}$F of CHClF$_2$ adsorbed on more basic zeolites LiX and NaX is similar to that of the free molecule, suggesting negligible cation–halogen interactions, and then, that the adsorption is driven by the zeolite basicity [50].

To summarize, the extent of the halogen–cation interactions for CHClF$_2$ and CHCl$_3$ will depend on the type of extra-framework cations and the zeolite basicity [50]. The interaction with the cation may prevent the use of CHClF$_2$ as a probe molecule for the quantification of basic centres.

### 3.3. Methanol

Methanol is adsorbed on alkali-exchanged zeolites giving rise to three structures with different infrared stretching vibration frequencies of the hydroxyl groups, $\nu$(OH) [31,32]; all them are dominated by the interaction between the oxygen atom of the hydroxyl groups (electron pair donor) and the alkaline cation (electron pair acceptor) [31,32]. The hydroxyl groups vibrates freely in high silica zeolites, giving a relatively sharp band I in the range 3620–3600 cm$^{-1}$ [31,32]. The basicity increase in zeolites with higher aluminium content, like faujasites X and Y, induces the simultaneous interaction of the hydrogen of the methanol hydroxyl group with the negatively charged lattice oxygen, appearing the $\nu$(OH) band II in the range 3450–3550 cm$^{-1}$ [31,32]. For more basic zeolites with higher concentration of alkali metal cations and adsorption sites, additional bonding among adsorbed methanol molecules gives rise to structure III, shifting the infrared $\nu$(OH) bands to lower frequencies [31,32]. Therefore, the presence of two low frequency bands in the range 3450–3210 cm$^{-1}$ in the spectra of more basic zeolites is attributed to adsorption sites with different basic strength (structure II), and/or to the occurrence of lateral interactions between the adsorbed methanol molecules (structure III) [31,32]. For more basic zeolites, more uniform and strongly hydrogen bonded sorption structures point to the formation of ring-like methanol structures [34].

Theoretical calculations show that the Lewis acidity of the cation determines the site and the energy of methanol adsorption, while the basicity of the adjacent framework oxygen atoms dominates the formation of the hydrogen bond [32]. This bonding contributes only moderately to the adsorption energy, but it significantly influences the infrared OH stretching frequency of adsorbed methanol [32]. The experimental frequency shifts of the infrared bands of structures II and III of zeolites NaY, NaX and partially exchanged KX correlate with the calculated proton affinity [32], as well as with the negative charge density on the lattice oxygen atoms calculated by the electronegativity equalization model, as shown in Fig. 11. However, we must note that the vibration frequency for CsX is much lower than expected (see Fig. 11), which can be tentatively related to the lower acidity of the bulky Cs$^+$ cation. Vayssilov and Rösch [33] proposed a method to estimate the proton affinity of a zeolite from the frequency shift of the $\nu$(OH) vibration of adsorbed methanol, taking advantage of the correlation existing between both properties. This method makes use of some equations derived after calibration of the proton

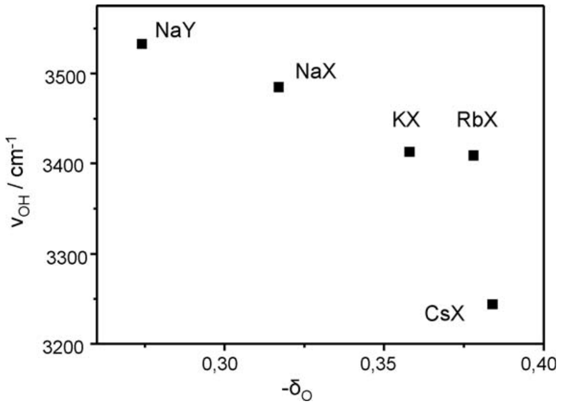

**Fig. 11.** Correlation of the stretching frequency of OH hydroxyl group of methanol, $\nu_{NH}$, adsorbed on different alkali-exchanged FAU-type zeolites versus the mean negative charge on the lattice oxygen atoms calculated by the electronegativity equalization method, after Ref. [31].

affinities calculated theoretically for a series of alkali-exchanged zeolites [33].

The hydrogen bonding between the proton of the methanol hydroxyl group and the lattice oxygen is supported by $^1$H NMR spectroscopy [35]. The resonance of the hydroxyl group of methanol and other alcohols adsorbed on alkali-exchanged zeolites shifts to low field as zeolite basicity increases [35]. Similar structures exist for all $C_1$–$C_4$ *n*-alcohols adsorbed on partially alkali-exchanged X zeolites, with the simultaneous hydrogen bonding of the hydrocarbon chain with the zeolite wall at low loading [35]. The $\nu$(OH) bands and the $^1$H chemical shifts of the OH resonances of adsorbed alcohols are only slightly different for a given zeolite, indicating that the interactions involved are quite independent on the chain length [35].

Theoretical calculations indicate that adsorption of methanol is influenced mainly by the identity of the alkali metal cation, whereas other factors such as the Si/Al ratio are of secondary importance [36]. In this same publication [36], it is concluded that cations are displaced only slightly by interaction with methanol, being those at SIII sites the more likely location for methanol activation.

## 4. Final remarks

In zeolites, the lattice oxygen atoms bearing the negative charge are Lewis basic sites, whereas the exchangeable cations act as Lewis acid sites, forming a conjugated acid–base pair which can interact with any molecule. An ideal probe molecule for zeolite basicity should adsorb selectively on basic lattice oxygen atoms and not induce any modifications in the solid. In this sense, the use of ‘in situ’ generated probe molecules such as $CH_3^+$ and $NO^+$, exclusively interacting with the framework oxygens, appear promising. However: (i) the zeolite network becomes compensated by $CH_3^+$ or by $NO^+$ instead of by the original alkali cation; (ii) the formation of halides and nitrates of alkaline cations (ionic salts, for instance NaI or $NaNO_3$ for $Na^+$-compensated zeolites) may modify the intrinsic strength of the basic centres. Nevertheless, though the usefulness of $NO^+$ is limited to some extent, methoxy groups appear as an appropriate NMR probe of basic properties of zeolite for a relatively large range of basicity.

The probe molecules forming hydrogen bonds with the framework basic oxygen atoms usually induce displacement of the cations from its original position, modifying somehow the charge distribution in the zeolite. The direct interaction of the molecule with the cations has been proved for pyrrole and halocarbons, and is the main contribution in the adsorption complexes of methanol (and other alcohols). Therefore, the simultaneous interaction with Lewis acidic cations seems to be difficult to avoid, and the goodness of a molecule to act as a probe for zeolite basicity will depend somehow on which interaction dominates.

The interaction of the adsorbate with alkaline cations predominates on the adsorption of alcohols (probably explaining the lack of correlation with the basicity of CsX), and is very weak for chloroform, whereas for chlorodifluoromethane is only dominant on some zeolites. The spectroscopic properties of pyrrole correlate well with zeolites basicity, and its advantages against chloroform are higher sensitivity, lower reactivity with temperature, and the detection of basic sites heterogeneity. This heterogeneity is originated by changes in the zeolite local composition, giving indirect information on the distribution of the $AlO_4$ tetrahedra in the framework of faujasites.

From the results reviewed here for several molecules (methoxy, nitrosonium, halocarbons, pyrrole and alcohols), it appears that there is no ideal probe molecule for zeolite basicity. Then, the proper chose among those proposed in the bibliography will be based on the similarity with the reactant molecules for a given process, or the good correlations in the adequate basicity range. Amongst the molecules reviewed here, pyrrole and the methoxy groups correlate well with the oxygen basicity for a relatively large range of zeolites basicities.

## Acknowledgments

Spanish CICYT (project MAT2006-08039) is acknowledged for financial support. MSS acknowledges the Spanish Ministry of Science and Innovation for a Ramon-y-Cajal contract.

## References

[1] (a) A. Corma, M.E. Davis, Chem. Phys. Chem. 5 (2004) 304;
(b) A. Corma, F. Rey, J. Rius, M.J. Sabater, S. Valencia, Nature 431 (2006) 287.
[2] A. Corma, J. Catal. 216 (2003) 298.
[3] H. Hattori, Chem. Rev. 95 (1995) 537.
[4] D. Barthoumeuf, Catal. Rev. Sci. Eng. 38 (1996) 521.
[5] (a) J. Weitkamp, M. Hunger, U. Rymsa, Micropor. Mesopor. Mater. 48 (2001) 255;
(b) J. Weitkamp, M. Hunger, Stud. Surf. Sci. Catal. 168 (2007) 787 (Introduction to Zeolita Science and Practice, 3rd revised edition).
[6] R.J. Davis, J. Catal. 216 (2003) 396.
[7] C. Laborde-Boutet, G. Joly, M. Thomas, P. Magnoux, Ind. Eng. Chem. Res. 45 (2006) 8111.
[8] M.K. Crawford, K.D. Dobbs, R.J. Smalley, D.R. Corbin, N. Maliszewskyj, T.J. Udovic, R.R. Cavanagh, J.J. Rusch, C.P. Grey, J. Phys. Chem. B 103 (1999) 431.
[9] J. Weitkamp, M. Fritz, S. Ernst, Int. J. Hydrogen Energy 20 (1995) 967.
[10] S.H. Jhung, J.W. Yoon, J.S. Lee, J.-S. Chang, Chem. Eur. J. 13 (2007) 6502.
[11] D. Barthomeuf, J. Phys. Chem. 88 (1984) 42.
[12] P.O. Scokart, P.G. Rouxhet, Bull. Soc. Chim. Belge. 90 (1981) 983.
[13] (a) D. Barthomeuf, Micropor. Mesopor. Mater. 66 (2003) 1;
(b) D. Barthomeuf, J. Phys. Chem. 109 (2005) 2047.
[14] M. Huang, S. Kaliaguine, J. Chem. Soc., Faraday Trans. 88 (1992) 751.
[15] (a) M. Huang, A. Adnot, S. Kaliaguine, J. Am. Chem. Soc. 114 (1992) 10005;
(b) M. Huang, A. Adnot, S. Kaliaguine, J. Catal. 137 (1992) 322.
[16] J.C. Lavalley, Catal. Today 27 (1996) 377.
[17] D. Murphy, P. Massiani, R. Franck, D. Barthomeuf, J. Phys. Chem. 100 (1996) 6731.
[18] D. Murphy, P. Massiani, R. Franck, D. Barthomeuf, Stud. Surf. Sci. Catal. 105 (1997) 639 (Progress in Zeolite and Microporous Materials).
[19] R. Heidler, G.O.A. Janssens, W.J. Mortier, R.A. Schoonheydt, Micropor. Mater. 12 (1997) 1.
[20] H. Förster, H. Fuess, E. Geidel, B. Hunger, H. Jobic, C. Kirschhock, O. Klepel, K. Krause, Phys. Chem. Chem. Phys. 1 (1999) 593.
[21] M. Sánchez-Sánchez, T. Blasco, Chem. Commun. (2000) 491.
[22] M. Sánchez-Sánchez, T. Blasco, J. Am. Chem. Soc. 124 (2002) 3443.
[23] J. Xie, M. Huang, S. Kaliaguine, React. Kinet. Catal. Lett. 58 (1996) 217.
[24] J. Xie, M. Huang, S. Kaliaguine, Appl. Surf. Sci. 115 (1997) 157.
[25] E. Bosch, S. Huber, J. Weitkamp, H. Knözinger, Phys. Chem. Chem. Phys. 1 (1999) 579.
[26] M. Sánchez-Sánchez, T. Blasco, F. Rey, Phys. Chem. Chem. Phys. 1 (1999) 4529.
[27] J.T. Timonen, T.T. Pakkanen, Micropor. Mesopor. Mater. 30 (1999) 327.
[28] C.F. Mellot, A.M. Davidson, J. Eckert, A.K. Cheetham, J. Phys. Chem. B 102 (1998) 2530.
[29] A.M. Davidson, C.F. Mellot, J. Eckert, A.K. Cheetham, J. Phys. Chem. B 104 (2000) 432.

[30] J. Eckert, C.M. Draznieks, A.K. Cheetham, J. Am. Chem. Soc. 124 (2002) 170.
[31] M. Repp, A.E. Palomares, G. Eder-Mirth, J.G. van Ommen, N. Rösch, J.A. Lercher, J. Phys. Chem. B 104 (2000) 8624.
[32] G.N. Vayssilov, J.A. Lercher, N. Rösch, J. Phys. Chem. B 104 (2000) 8614.
[33] G.N. Vayssilov, N. Rösch, Phys. Chem. Chem. Phys. 4 (2002) 146.
[34] R. Schenkel, A. Jentys, S.F. Parker, J.A. Lercher, J. Phys. Chem. B 108 (2004) 7902.
[35] R. Schenkel, A. Jentys, S.F. Parker, J.A. Lercher, J. Phys. Chem. B 108 (2004) 15013.
[36] D.F. Plant, A. Simperler, R.G. Bell, J. Phys. Chem. B 110 (2006) 6170.
[37] V. Bosáček, J. Phys. Chem. 97 (1993) 10732.
[38] V. Bosáček, R. Klik, G. Genoni, G. Spano, F. Rivetti, F. Figueras, Magn. Reson. Chem. 37 (1999) S135.
[39] M. Hunger, U. Schenk, B. Burger, J. Weitkcamp, Angew. Chem., Int. Ed. Engl. 36 (1997) 2504.
[40] U. Schenk, M. Hunger, J. Weitkamp, Magn. Reson. Chem. 37 (1999) S75.
[41] P. Mignon, P. Geerlings, R. Schoonheydt, J. Phys. Chem. B 110 (2006) 24947.
[42] F. Thibault-Starzyk, O. Marie, N. Malicki, A. Vos, R. Schoonheydt, P. Geerlings, C. Henriques, C. Pommier, P. Massiani, Stud. Surf. Sci. Catal. 158 (2005) 663 (Molecular Sieves: From Basic Research to Industrial Applications).
[43] O. Marie, N. Malicki, C. Pommier, P. Massiani, A. Vos, R. Schoonheydt, P. Geerlings, C. Henriques, F. Thibault-Starzyk, Chem. Commun. 1049 (2005).
[44] B. Gil, K. Mierzynska, M. Szczerbinska, J. Datka, Appl. Catal. A: Gen. 319 (2007) 64.
[45] A.M. Vos, P. Mignon, P. Geerling, F. Thibault-Starzyk, R.A. Schoonheydt, Micropor. Mesopor. Mater. 90 (2006) 370.
[46] E.A. Pidko, P. Mignon, P. Geerlings, R.A. Schoonheydt, R.A. van Santen, J. Phys. Chem. C 112 (2008) 5510.
[47] P. Mignon, E.A. Pidko, R.A. Van Santen, P. Geerlings, R.A. Schoondeydt, Chem. Eur. J. 14 (2008) 5168.
[48] (a) M. Sánchez-Sánchez, T. Blasco, Stud. Surf. Sci. Catal. 135 (2001) 1913 (Zeolites and Mesoporous Materials at the Dawn of the 21st Century);
(b) M. Sánchez-Sánchez, J.A. Vidal-Moya, T. Blasco, Stud. Surf. Sci. Catal. 154 B (2004) 1769 (Recent Advances in the Science and Technology of Zeolites and Related Materials).
[49] M. Sánchez-Sánchez, A. Vidal-Moya, T. Blasco, Stud. Surf. Sci. Catal. 138 (2001) 223 (Spillover and Mobility of Species on Solid Surfaces).
[50] M. Sánchez-Sánchez, T. Blasco, A. Corma, J. Phys. Chem. C 112 (2008) 16961.
[51] D.K. Murray, J.-W. Chang, J.F. Haw, J. Am. Chem. Soc. 115 (1993) 4732.
[52] C. Henriques, O. Marie, F. Thibault-Starzyk, J.C. Lavalley, Micropor. Mesopor. Mater. 50 (2001) 167.
[53] K. Hadjiivanov, J. Saussev, J.L. Frevsz, J.C. Lavalley, Catal. Lett. 52 (1998) 103.
[54] G.F. Smith, Adv. Heterocycl. Chem. 2 (1963) 287.
[55] G. Spoto, F. Geobaldo, S. Bordiga, C. Lamberti, D. Scarano, A. Zecchina, Top. Catal. 8 (1999) 279.
[56] P.O. Scokart, P.G. Rouxhet, J. Chem. Soc., Faraday I 76 (1980) 1476.
[57] J.C. Lavalley, Trends Phys. Chem. 2 (1991) 305.
[58] C. Binet, A. Jadi, J. Lamotte, J.C. Lavalley, J. Chem. Soc., Faraday Trans. 92 (1996) 123.
[59] J. Hine, A.M. Dowell Jr., J.E. Singley Jr., J. Am. Chem. Soc. 78 (1956) 479.
[60] E.A. Paukshits, E.N. Yurchenko, Russ. Chem. Rev. 52 (1983) 242.
[61] I. Hannus, Z. Koanya, J.B. Nagy, P. Lentz, I. Kiricsi, Appl. Catal. B: Environ. 17 (1998) 157.
[62] M. Katoh, H. Hatayama, T. Yamazaki, S. Ozawa, Nippon Kagaku Kaishi (1997) 24.
[63] A. Kogelbauer, C. Gründling, J.A. Lercher, J. Phys. Chem. 100 (1996) 1852–1857.
[64] (a) A. Philippou, M.W. Anderson, J. Am. Chem. Soc. 116 (1994) 5774;
(b) M. Hunger, U. Schenk, J. Weitkamp, J. Mol. Catal. A: Chem. 134 (1998) 97.
[65] R.J. Corrêa, Tetrahedron Lett. 44 (2003) 7299.
[66] E.A. Pauskshits, N.S. Kotsarenko, L.G. Karakchiev, React. Kinet. Catal. Lett. 12 (1979) 315.
[67] P. Berteau, M.A. Kellens, B. Delmon, J. Chem. Soc., Faraday Trans. 87 (1991) 1425.
[68] S. Huber, H. Knözinger, J. Mol. Catal. A 141 (1999) 117.
[69] A.A. Davidov, M.L. Shepot'ko, A.A. Budneva, Kinet. Katal. 35 (1994) 299.
[70] E.B. Uvarova, L.M. Kustov, V.B. Kazansky, Stud. Surf. Sci. Catal. 94 (1995) 254 (Catalysis by Microporous Materials).
[71] N.A. Ramsahye, R.G. Bell, J. Phys. Chem. B 109 (2005) 4738.
[72] M. Yoshikawa, T. Yoshida, M. Ishiwata, T. Hasegawa, S. Ozawa, Adsorption 3 (2000) 259.
[73] A. Chatterjee, T. Ebina, T. Iwasaki, F. Mizukami, J. Mol. Struct. (Theochem) 630 (2003) 233.